Journal of Environmental Management 92 (2011) 2504–2512

Contents lists available at ScienceDirect

Journal of Environmental Management

journal homepage: www.elsevier.com/locate/jenvman

An Assessment of U(VI) removal from groundwater using biochar produced from hydrothermal carbonization

Sandeep Kumar [a,1], Vijay A. Loganathan [b,1], Ram B. Gupta [c], Mark O. Barnett [d,*]

[a] Department of Civil and Environmental Engineering, Old Dominion University, Norfolk, VA 23529, USA
[b] Environmental Sciences Division, P.O. Box 2008, MS 6038, Oak Ridge National Laboratory, Oak Ridge, TN 37831 6038, USA
[c] Department of Chemical Engineering, Auburn University, Auburn, AL 36849-5127, USA
[d] Department of Civil Engineering, Auburn University, Auburn, AL 36849-5127, USA

ARTICLE INFO

Article history:
Received 10 August 2010
Received in revised form
2 May 2011
Accepted 8 May 2011
Available online 12 June 2011

Keywords:
Hydrothermal carbonization
Biochar
Uranium
Adsorption
Remediation
Permeable reactive barrier

ABSTRACT

The ever-increasing growth of biorefineries is expected to produce huge amounts of lignocellulosic biochar as a byproduct. The hydrothermal carbonization (HTC) process to produce biochar from lignocellulosic biomass is getting more attention due to its inherent advantage of using wet biomass. In the present study, biochar was produced from switchgrass at 300 °C in subcritical water and characterized using X-ray diffraction, fourier transform infra-red spectroscopy, scanning electron micrcoscopy, and thermogravimetric analysis. The physiochemical properties indicated that biochar could serve as an excellent adsorbent to remove uranium from groundwater. A batch adsorption experiment at the natural pH (~3.9) of biochar indicated an H-type isotherm. The adsorption data was fitted using a Langmuir isotherm model and the sorption capacity was estimated to be ca. 2.12 mg of U g^{-1} of biochar. The adsorption process was highly dependent on the pH of the system. An increase towards circumneutral pH resulted in the maximum adsorption of ca. 4 mg U g^{-1} of biochar. The adsorption mechanism of U(VI) onto biochar was strongly related to its pH-dependent aqueous speciation. The results of the column study indicate that biochar could be used as an effective adsorbent for U(VI), as a reactive barrier medium. Overall, the biochar produced via HTC is environmentally benign, carbon neutral, and efficient in removing U(VI) from groundwater.

1. Introduction

The contamination of groundwater due to the naturally occurring radioactive element, uranium, is a serious matter of concern. The issue of long-term stewardship of uranium contaminated sites, e.g., some of the U.S. Department of Energy sites contaminated with uranium (Davis et al., 2004) and the major nuclear reactor accidents emphasize the need for research in remedial actions for uranium contamination. Moreover, contamination of uranium by groundwater is a global environmental problem as countries increasingly move towards cleaner energy sources (Srivastava et al., 2010). Uranium, a radiotoxic element also possesses risk related to chemical toxicity. Among the various oxidation states of uranium, IV and VI oxidation states are the most important states in geological environments (Ervanne, 2003). The chemical toxicity of uranium is predominantly caused by the highly reactive hexavalent uranyl ions (Vandenhovea et al., 2006).

In the last few years, biosorption of radionuclides by different raw biomasses such as cork, rice and tea leaves, straw, coco shaving, coir pith, peat moss, etc. have been increasingly studied (Parab et al., 2005; Psarevaa et al., 2005). Numerous other materials such as zeolite (Camacho et al., 2010), hematite (Zeng et al., 2009), diatomite (Aytas et al., 1999), etc. have also been tested for the same purpose. Activated carbon, a form of high temperature biochar that has been treated with steam or CO_2 to maximize porosity, is the oldest and most widely used adsorbents (Mellah et al., 2006; Suhas and Carrott, 2007). However, this adsorbent is relatively expensive owing to its higher production cost associated with the activation process (Savovaa et al., 2001).

Biochar, which is a byproduct of biorefineries, has attracted much attention recently due to its proven role in environmental management issues. In view of the government focus on renewable and alternative fuels, the biofuel industry of the US is on a tremendous growth path. In fact, Renewable Fuel Standard (RFS) as part of Energy Independence and Security Act (EISA) of 2007

* Corresponding author. Tel.: +1 334 844 6291; fax: +1 334 844 6290.
E-mail address: mark.barnett@auburn.edu (M.O. Barnett).
[1] Both the authors contributed equally to this work.

0301-4797/$ – see front matter © 2011 Elsevier Ltd. All rights reserved.
doi:10.1016/j.jenvman.2011.05.013

requires 36 billion gallon per year (BGY) of biofuels by 2022 (National Biofuels Action Plan, 2008). In this scenario, the abundantly available lignocellulosic biomasses are being considered as the major biomass feedstock. Moreover, the billion ton vision report concludes that the land resources of the US are capable of producing a sustainable supply of biomass (Perlack et al., 2005).

Biomass may be converted to fuels by many different thermochemical processes such as gasification, pyrolysis, hydrothermal liquefaction/carbonization (Kumar and Gupta, 2009). Biochar, a non-liquefied carbonaceous solid byproduct that results from the thermochemical conversion processes has been extensively studied for their application as a soil amendment (Laird et al., 2009; Gaunt and Lehmann, 2008).

The yield of biochar (Table 1) mainly depends on the processing condition and type of biofuels being produced. The properties and composition of biochar change based on the production routes. For example, ash contents are higher in biochar produced from gasification/pyrolysis routes, whereas hydrothermally produced biochars are richer in carbonaceous materials. Through hydrothermal carbonization (HTC), a carbon-rich black solid is obtained from biomass as an insoluble product in the temperature range of 180–350 °C (Savovaa et al., 2001; Titirici et al., 2007). Furthermore, during the process of biochemical conversion of biomass for bioethanol production, lignin-rich wet residues are generated which may be potentially converted to biochar. This is an environmentally friendly process because of its mere simplicity of using water as the sole reaction medium under pressure and heat, that leaves no further hazardous chemical waste or by product (Hu et al., 2008). It has attracted much attention due its versatility to utilize mixed biomass feedstock without any pretreatment or drying, at a comparatively low temperature (Kumar and Gupta, 2009).

Biochar is porous with oxygen functional groups and aromatic surfaces. Biochar produced from lignocellulosic biomass has potential to adsorb both organic pollutants and heavy metals. Because of its high surface-to-volume ratio and strong affinity to nonpolar substances such as PAHs, dioxins, furans etc. biochar can be a potential sorbent for organic pollutants and pesticides, particularly planar aromatic compounds (Shrestha et al., 2010; Yu et al., 2009). Studies have been reported on the use of biochar for removing metal contaminants such as lead, mercury, and arsenic from aqueous solution (Amuda et al., 2007; Budinova et al., 2006; Kalderis et al., 2008). Biochar derived from dairy manure was reported to sorb both heavy metals and organics (Cao et al., 2009). Biochar strongly adsorbs dissolved organic compounds from soil solution and makes them less bioavailable (Laird et al., 2009; Loganathan et al., 2009). In fact, pyrogenic organic matters (e.g. biochar, charcoal, soot and activated carbon) have been studied extensively for their high affinity and capacity for absorbing organic compounds especially. Polycyclic aromatic hydrocarbons (PAH) (Smernik, 2009). High molecular weight PAH shows high affinity for biochar (Dachs, 2000). The study showed that adsorption of aromatic contaminants to wood char was assisted by π-electron interactions and pore-filling mechanism (Chen and Chen, 2009). Moreover, nonpolar (naphthalene) and polar (nitrobenzene, *m*-dinitrobenzene, and 1-naphthol) aromatic compounds were used to understand the sorption mechanism of biochar produced at different pyrolytic temperatures (Chen and Chen, 2009; Chen et al., 2008).

Table 1
Biochar yield from thermochemical conversion processes of biomass.

Process	Temperature and Time	Biochar Yield (%)	Reference
Gasification	750 °C, ~10–20 s	10	Brown, 2008
Pyrolysis			
• Fast	500 °C, ~1 s	12	Winsley, 2007
• Moderate	500 °C, ~10–20 s	20	Brown, 2008; Winsley, 2007
• Slow	500 °C, ~ 5–30 min.	35	Karaosmanoglu et al., 2000; Winsley, 2007
• Flash Carbonization	>400 °C	40–45	Antal et al., 2003
Hydrothermal Carbonization	250–350 °C, 10–60 min	45–60	Funke and Ziegler, 2010

Though the scientific literature is replete with the use of biochar as an adsorbent for environmental pollutants, these studies deal with organic contaminants. Relatively fewer studies have reported on the use of biochar for removing metal contaminants. Recently, Liu et al. (2010) have characterized the biochar produced via HTC (at 300 °C) and pyrolysis process (at 700 °C) and compared their adsorption capacity for copper ions. In the light of above work, the hypothesis of this study is that the hydrothermally produced biochar contain oxygen-rich functional groups on its surface and so are expected to show better affinity towards adsorption of dissolved U(VI). As U(VI) is one of the major pollutants of concern in many U.S. Department of Energy sites, and the lack of thorough literature on U(VI)-biochar interaction, a study of this nature is warranted to provide better alternative remediation technologies.

Switchgrass, a summer perennial grass native to North America that grows on marginal land, is considered to be a major energy crop of interest for the second generation biofuels. It is an immense biomass producer that can reach heights of ≥10 feet and provide 6-8 dry-tons/acre/year yields with a high cellulosic content. Though switchgrass is being extensively studied for the production of biofuels, there is no previous study on using switchgrass biochar as sorbent for treating radionuclide contaminants. The major objective of this work was to assess the adsorption of uranium onto biochar produced from switchgrass by HTC. The specific objective of this study was to investigate the use of this environmentally friendly and benign sorbent for treating uranium contaminated groundwater.

2. Experimental section

Switchgrass that was chopped to 5–10 mm length was reacted with de-ionized water to produce biochar. Conversion of switchgrass to biochar was conducted in a high- pressure batch reactor. The apparatus consisted of a 500 mL high temperature, high-pressure metal reactor equipped with proportional-integral-differential controllers. Biomass and water (7:1) were charged into the reaction vessel and the reactor temperature was raised to 300 °C with a heating rate of 7 °C min^{-1}. After maintaining the temperature at 300 °C for 30 min under autogeneous pressure conditions, the reactor was rapidly cooled to ambient conditions using water through a cooling coil. The product biochar was separated from the liquid after the reaction and further washed with deionized water. Three separate experiments were conducted to produce biochar under the same process condition at 300 °C for confirming the reproducibility of the process. The resulting biochar was air dried and used for further characterization.

The physical and chemical characteristics of biochar were examined by X-ray diffraction (XRD), elemental analysis, thermogravimetric analysis (TGA), fourier transform infra-red spectroscopy (FTIR), and scanning electron microscopy (SEM) techniques. Batch adsorption studies were designed to assess the sorption potential of biochar for U(VI). The study examines the adsorption kinetics and equilibrium, and the effect of solid (biochar) loading and pH on U(VI) adsorption. In addition, the feasibility of biochar as a permeable reactive barrier medium was investigated using column experiments.

3. Product characterization

3.1. Elemental analysis

Both switchgrass and biochar samples were dried in a forced-air oven at 60 °C. About 0.1–0.2 g of each sample was weighed into tin foil cups and combusted with an oxygen catalyst at 1150 °C. The total carbon was measured by the thermal conductivity method (Kirsten, 1979) using an Elementar Vario Macro CNS analyzer. For quantifying macro and micronutrients and metals, approximately 1.0 g of dried sample was weighed into ceramic crucibles. The samples were then ashed for 8 h in a muffle furnace at 500 °C. This was followed by digestion on a hot plate using 1 N HNO_3 and 1 N HCl. Finally, the digested samples were filtered into 50 mL volumetric flasks and brought to volume with deionized water. All samples were analyzed using a Varian Vista-MPX Axial Spectrometer (Isaac and Johnson, 1985). Analysis was set for 2 exposures (repetitions) per sample and the average results were recorded.

3.2. SEM analysis

The samples were held onto adhesive carbon tape on an aluminum stub followed by sputter coating with gold. Surface morphology of the sample was studied using an environmental scanning electron microscopy system (Zeiss EVO 50).

3.3. XRD analysis

Rigaku Miniflex powder X-ray diffractometer equipped with a Cu $K\alpha_1$ radiation source at 30 kV voltages, 15 mA current and a miniflex goniometer was used for the XRD analysis. Diffraction patterns were collected in the 2θ range of 12–35° at a scan speed of 1° min^{-1} and a step size of 0.05°.

3.4. FTIR analysis

Infrared spectra (4000–400 cm^{-1}) were recorded using a Nicolet IR100 FTIR spectrometer that was equipped with a TGS/PE detector and a silicon beam splitter with 1 cm^{-1} resolution. The sample discs were prepared by mixing oven-dried (at 105 °C) samples with spectroscopy-grade KBr in an agate mortar.

3.5. BET surface area measurement

The method of Brunauer, Emmett, and Teller (BET) is commonly used to determine the total surface area of materials. The BET analysis was carried out using NOVA 2200e surface area and pore size analyzer (Quantachrome Instruments). Raw switchgrass and biochar samples were analyzed for multipoint BET surface area using nitrogen as the adsorbing gas at 77 K. The analysis involved outgassing the switchgrass samples at 105 °C for 3 h and biochar samples at 75 °C for 22 h. In the case of biochar, the pore volume and pore radius was measured along with surface area. Selected samples were analyzed in duplicate and the results agreed within 5%.

3.6. Thermogravimetric analysis (TGA)

TGA was conducted using a TGAQ 5000 instrument under a high-purity (99.99%) helium gas flow. Samples were placed in a sample pan and heated from room temperature to 700 °C at a heating rate of 10 °C min^{-1}. The TGA curves were obtained directly from the apparatus while the derivative thermogravimetric (DTA) curves were obtained by the software Universal V4.3A.

4. Adsorption studies

4.1. Batch adsorption kinetic experiments

Batch kinetic experiments were performed at two different solid-to-solution ratios (SSR: 4 and 5 g L^{-1}) and initial U(VI) concentrations (ca. 30 and 10 mg L^{-1}) to estimate the equilibrium time for the adsorption reaction. The experiments were performed at the natural pH of biochar (ca. pH 3.9 ± 0.2) with 0.1 M $NaNO_3$ as the background solution. The experiments were carried out for 72 h and samples were taken at regular intervals by sacrificing the tubes. U(VI) was measured using a kinetic phosphorescence analyzer (KPA, Chemchek Instruments, Inc.) after filtration of the samples through 0.45 μm polytetrafluoroethylene filter units and acidifying the samples to pH 1.0. The difference between the initial U(VI) concentration and aqueous U(VI) concentration was attributed to the adsorption of U(VI) onto biochar. Both the experiments had duplicate test tubes for each sampling interval, blanks [no U(VI)], and controls (no biochar).

4.2. Batch adsorption equilibrium experiment

A batch isotherm experiment was performed at a solid loading of 5 g L^{-1} and at a pH of 3.9 ± 0.2. The initial concentration of U(VI) was varied between 5 and 30 mg L^{-1} and the experiment was conducted in a 0.1 M $NaNO_3$ background solution. Moreover, to study the effect of solid-to-solution ratio on adsorption, biochar was loaded at 1 g L^{-1} containing an initial U(VI) concentration of 10 mg L^{-1}. The test tubes were prepared in duplicates and tumbled for about 34 h at 25 °C. At the end of the equilibrium time, aqueous samples were filtered and acidified and analyzed as described above. Similar to the kinetic experiments, the difference between the initial U(VI) concentration and aqueous U(VI) concentration was attributed to the adsorption of U(VI) onto biochar. Further, the pH-dependent adsorption of U(VI) onto biochar was also studied by varying the pH (3–8).

4.3. Permeable reactive barrier (PRB) experiment

Approximately 0.25 g of biochar was packed into a 1.0 cm × 10 cm glass column as an interlayer of about 0.8 cm depth between two quartz zones of 0.6 cm and 5.4 cm. The column was initially flushed with the background solution, 0.1 M $NaNO_3$, adjusted to pH 3.9 ± 0.2 at a flow rate of 4.1 mL h^{-1}. After a few pore volumes of $NaNO_3$ flushing, U(VI), prepared in 0.1 M $NaNO_3$, and adjusted to pH 3.9 ± 0.2, at an initial concentration of ca. 3 mg L^{-1} was flushed through the column. Samples were collected at regular intervals and the pH was checked frequently. A stable pH of about 3.9 ± 0.2 was maintained in the effluent solution throughout the course of the experiment. At the end of the biochar site saturation, which was estimated based on the batch experiment results, the influent solution was changed back to U(VI)-free $NaNO_3$. A control for the permeable reactive barrier column was simultaneously run wherein the entire column was packed with pure white quartz with a particle size ranging between 0.210 and 0.297 mm, which was pre-washed with 0.1 M nitric acid. The experimental protocol for the control column was similar to the PRB column except for it was fully packed (6.8 cm) with pure quartz. In the case of the control column, a stable pH of 3.9 ± 0.2 was also maintained in the effluent solution throughout the course of the experiment. The residence time for the control column was calculated to be ca. 76.4 min whereas, in the case of PRB column, the residence for the PRB zone (0.8 cm) was ca. 8.99 min. At the end of the experiments selected samples were acidified and analyzed for U(VI) in KPA.

Table 2
Composition of switchgrass and biochar.

Elements	C (wt%)	Ash	Ca (ppm)	K	Mg	P	Fe	Mn	Na	Pb
Switchgrass	44.6	4.5	2105	4082	4514	941	115	48	701	1
Biochar	70.5	3.7	2029	665	2215	481	258	53	395	<0.1

5. Results and discussion

5.1. Product characterization

The oxygen content in raw switchgrass is typically 40–43 wt% (Berg and Visser, 2001), which was reduced to about 22–23 wt% in biochar. The elemental carbon in biochar was increased to 70.5 wt% compared to switchgrass that had 44.6 wt% (Table 2). Though the ash content did not change significantly, some of the inorganic compounds (e.g. K, Mg, P, and Na) decreased due to their solubilization in subcritical water. As result of carbonization process in subcritical water, more than 70 wt% of oxygen present in switchgrass could be removed and the product biochar became richer in carbon content. The formation of the carbon-rich solid through the carbonization of biomass in water medium is the consequence of dehydration, condensation, polymerization, and aromatization reactions (Funke and Ziegler, 2010). The biochar yield (dry weight basis) and higher heating value (measured in a IKA-C200 Calorimeter) of biochar produced from switchgrass was 42.9 wt% and 28.7 MJ/kg on an oven-dry basis. The relative standard deviation of biochar yield and its heating value were 3.3% and 1.1%, respectively. The effect of temperature, pressure, and residence time on the yield and the oxygen-to-carbon ratio (O/C) of biochar has been studied separately (Kumar, 2010). The study showed that reaction temperature has more influence on the carbonization process compared to the effect of reaction time and pressure. With an increase in temperature, the mass yield of biochar decreased, but the heating value increased.

Typically, at higher temperatures dehydration reactions start dominating though water is present in excess in the reactor resulting in lower O/C ratios of the biochar (Patrick et al., 2001). The O/C ratio of switchgrass is about 0.9, which decreased to 0.37 for the biochar produced at 300 °C in subcritical water. The SEM images for switchgrass and biochar are shown in the Fig. 1. These images indicated that biochar has different macromolecular structure than raw switchgrass, and the average particle sizes became smaller after treatment. Further, the images show that biochar has an irregular surface and porous structure compared to raw switchgrass. These results are reflected in the higher surface area of biochar when compared to raw switchgrass. The specific surface area of switchgrass and biochar were 1.0 and 2.9 $m^2\ g^{-1}$, respectively. It has been reported that char surface area greatly depended on treatment temperature (Liu et al., 2010). Due to the high temperature and long residence time of the reaction conditions, the porous structure of biochar was cracked and the pores were partially blocked as a result of the repolymerization/recondensation of water soluble compounds. This could have resulted in the lesser increase in surface area for biochar. The total pore volume of the biochar was found to $7.2 \times 10^{-3}\ cm^3\ g^{-1}$ with an average pore radius of 50.02 Å, indicating that it is rich in micropores.

The cross-linked structure, which was made up of cellulose, hemicellulose, and lignin in switchgrass, was broken through fragmentation, decarboxylation, and dehydration reaction in subcritical water. Here, water acts as both a reactant and the reaction medium. Water as a reactant leads to hydrolysis reactions and rapidly degrades the polymeric structure of biomass. With the removal of polymeric components during the reactions, additional pores and terrains were created. The XRD patterns for switchgrass and biochar showed distinct sharp crystalline cellulosic peak at $2\theta = 22.7°$ (Fig. S1, supporting information). This peak comes from the crystal structure of cellulose (Segal et al., 1959) and was displayed in switchgrass, whereas it was absent in the biochar. The absence of any crystalline peak of cellulose in the biochar XRD pattern confirms that it contained mainly the amorphous components as a result of decomposition of cellulose.

The biochar was characterized by FTIR in the near IR region (wave number: 4000–400 cm^{-1}). A typical FTIR spectrum of biochar is shown in Fig. 2. Various band assignments in the FTIR spectrum for the samples are listed in Table S1 (supporting information). The change in absorbance peaks mainly appeared in the range of 1800 − 800 cm^{-1}. The FTIR spectrum of biochar was similar to that of switchgrass with respect to the peaks of lignin. The ether linkages present in switchgrass around 1200 cm^{-1} and 1000 cm^{-1} between the cellulose skeleton units were hydrolyzed. As seen in the spectra, most of the lignin fractions were retained

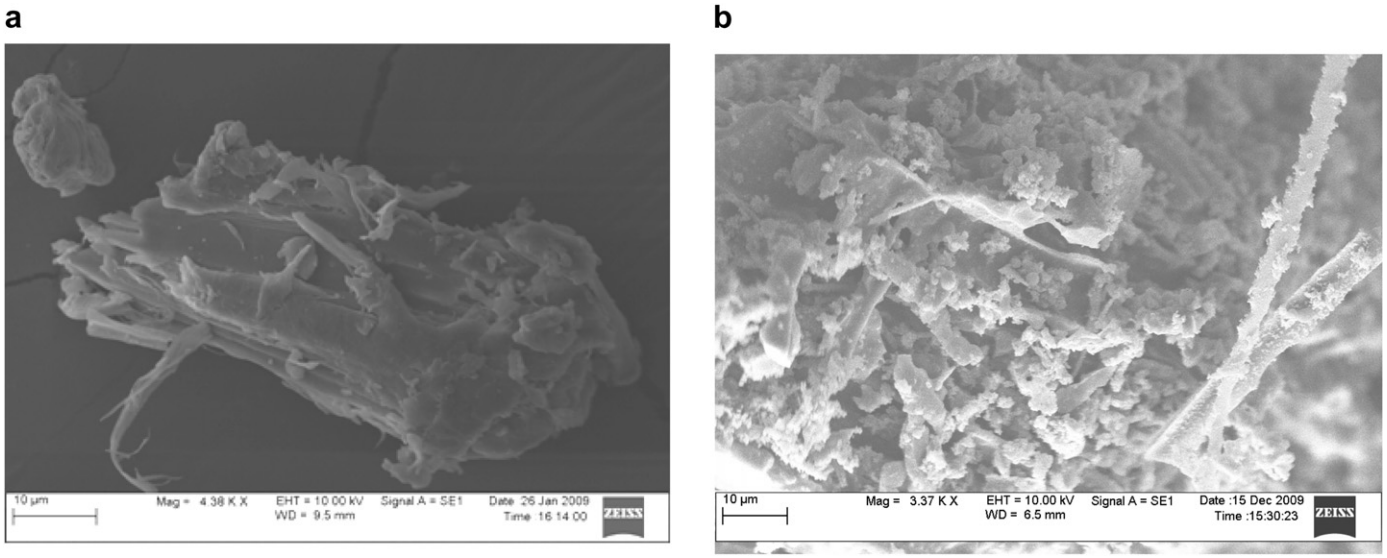

Fig. 1. SEM image of switchgrass (a), and biochar (b).

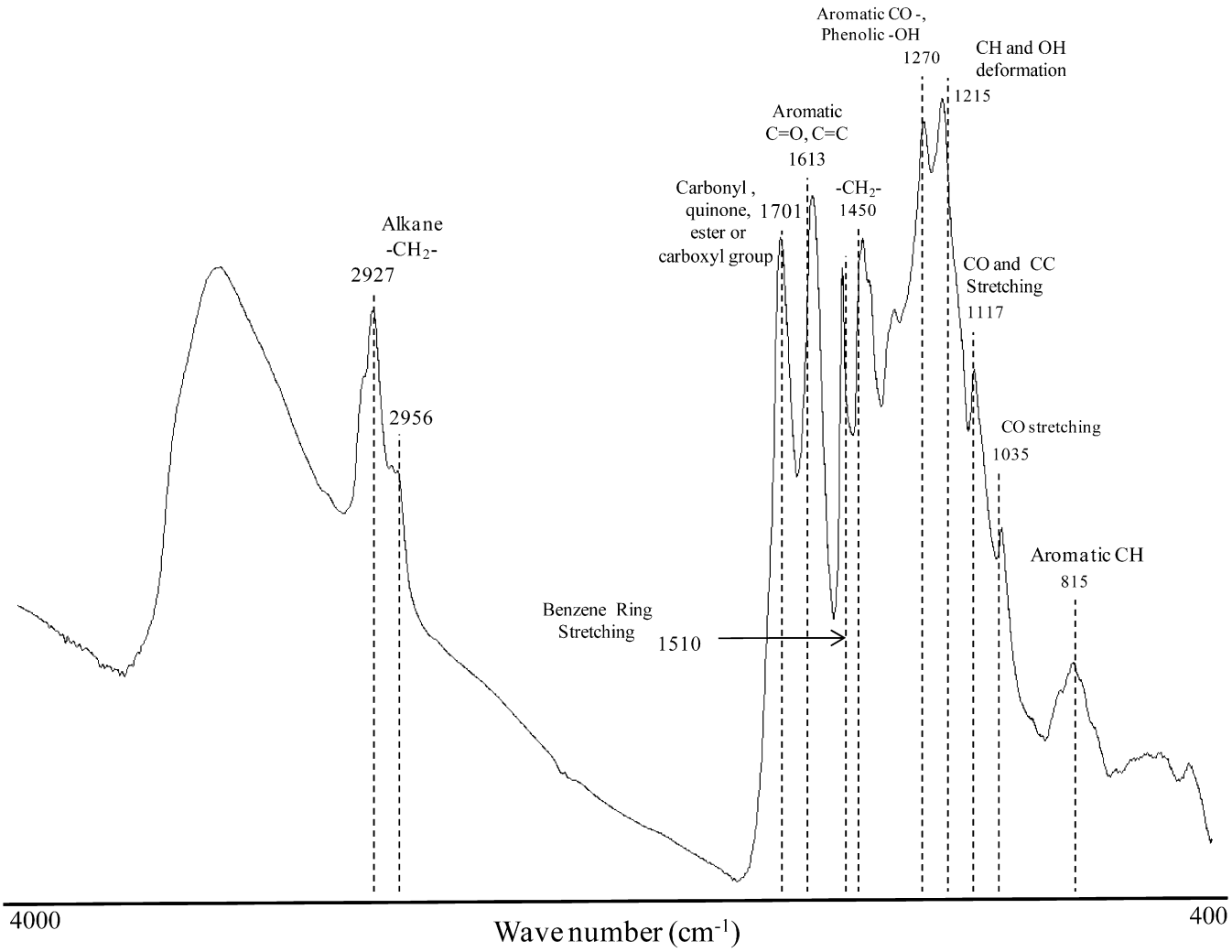

Fig. 2. FTIR spectrum of biochar.

in the biochar. The results were confirmed by the lignin peaks at 1270, 1424 and 1510 cm^{-1} in the FTIR. In addition, at 1613 and 1701 cm^{-1}, the peaks of polymeric product were also seen in the spectra. The results indicate that biochar is composed mainly of aromatic cores derived from the lignin fraction and polymeric product that was produced in the hydrothermal carbonization process. The peak at 893 cm^{-1} is characteristic of β-anomers or β-linked glucose polymers and the peak at 1053 cm^{-1} is C–O stretching. These peaks are present in the switchgrass but are absent in biochar. Further, the absence of a peak around 1635 cm^{-1} indicated that the moisture retention capability of biochar has drastically reduced (Baeza and Freer, 2001; Cheng et al., 2009; Kobayashi et al., 2009). The presence of several oxygen functional groups (carboxylic, hydroxyl/phenolic, carbonyl) in biochar are confirmed from the FTIR spectra.

As observed in the FTIR analysis, the presence of oxygen-rich organic compounds on the biochar surfaces adds substantial cation exchange capacity. For example, the biochar-amended soil has been reported to have 5–20% higher cation exchange capacity during a 500-day soil column leaching/incubation study conducted by Laird et al. (2009). Carboxylic groups present and also formed over time on the surface of biochar increases its nutrient holding capacity and also reduce the leaching of pollutants such as dissolved phosphates and nitrates into groundwater. The nanoporous structure of biochar with available oxygen functional groups on the surface provides an excellent opportunity to adsorb heavy metal ions from the aqueous solution (Hu et al., 2008; Sevilla and Fuertes, 2009; Tan et al., 1993). Typically, hydrothermally produced biochar has relatively more O/C and hydrogen-to-carbon (H/C) ratio and undergoes lesser carbonization processes compared to the biochar produced via pyrolysis process.

Biochar produced at higher temperature showed high pH, cation exchange capacity and surface area (Lehmann, 2007). On the contrary, biochar produced at low temperature showed availability of more actives sites and the existence of stable carbon–oxygen complexes. In a recent study on the HTC of model compound cellulose (a major component of lignocellulosic biomass), Sevilla and Fuertes (2009) showed that biochar consists of a high amount of oxygen (22–23 wt%) that is present in the core and in the shell of carbonaceous particles. Their analysis concluded that oxygen in the inner part probably consists of less reactive groups (i.e. ether, quinone, pyrone), whereas the shell contains more reactive/hydrophilic groups (i.e. hydroxyl, carbonyl, carboxylic, ester).

Thermogravimetric (TG) and derivative thermogravimetric (DTG) analyses were conducted under helium gas flow to understand the thermal stability of materials up to 700 °C (Fig. S2, supporting information). Weight loss in switchgrass was observed over

a wide range of temperature up to 700 °C, but the majority of weight loss (70%) occurred between 200 and 400 °C. The rapid weight loss below 400 °C is mainly because of the decomposition of holocellulose fractions of the switchgrass (Chen and Chen, 2009). On the contrary, the weight loss in biochar was relatively gradual up to 700 °C. In fact, nearly 45% of biochar remained even at 700 °C, which confirmed the thermal stability of biochar relative to the switchgrass. Raw biomass such as peat, poplar sawdust, and coconut shells have also been reported to show affinity towards metal ions particularly at low ion concentrations (McKay, 1997; Sciban et al., 2007). However, the use of raw biomass as adsorbents is associated with the risk of leaching of the organic pollutants due to the presence of extractable compounds. As supported by the TG analysis, biochar, which is more thermally stable as an adsorbent, will avoid such risks.

5.2. Batch adsorption results

The kinetic experiments indicated about 90% of initial U(VI) adsorption resulting within 8 h, at both solid-to-solution ratios (Fig. 3a). A similar fast adsorption reaction was reported for Pb (II) sorption onto biochar produced via HTC (Liu and Zhang, 2009). Based on the reaction kinetics, about 34 h of equilibrium time was chosen for the batch isotherm experiments. The batch adsorption isotherm is shown in Fig. 3b. The adsorption of U(VI) onto biochar followed an H-type isotherm (Limousin et al., 2007). A complete adsorption of 10 mg L^{-1} of initial U(VI) by 0.1 g of biochar was observed, beyond which the adsorption plateaus sharply. The shape of the isotherm indicates that this could have been due to the binding of uranyl cation onto biochar sites/pores. Once the adsorption sites get completely filled, the biochar ceases to adsorb more uranium resulting in a plateau. The adsorption data was fitted using a Langmuir isotherm model (Fig. 3c) and the sorption capacity of biochar was estimated to be ca. 2.12 mg U g^1 of biomass (0.2% w/w). Moreover, a similar distribution coefficient [K_d, where $K_d = q_e/c_e$; q_e (mg g^{-1}) is the equilibrium adsorbed-phase concentration and c_e (mg L^{-1}) is the equilibrium aqueous-phase concentration] was observed over a range of solid loading indicating a constant amount of adsorption sites in biochar structure (Fig. S3, supporting information). At the end of the batch sorption experiment, biochar was recovered, dried, and tested for crystalline peaks under x-ray diffraction. Lack of sharp peaks in the diffraction spectra suggested an adsorption phenomena rather than U(VI) precipitation. When compared to the studies reported on other heavy metals [Cu(II), Pb(II)], U(VI), the adsorption onto biochar showed similar adsorption potential (Liu and Zhang, 2009; Liu et al., 2010).

The adsorption of uranium was highly dependent on the solution pH. The pH edges (Fig. 3d) indicated that a unit increase in pH from 3.9 (natural pH of biochar) to 4.8 would result in ~100% more U(VI) adsorption. Hence, a maximum adsorption of about 90% of U(VI) occurred at about pH 5.9. Increasing the pH beyond

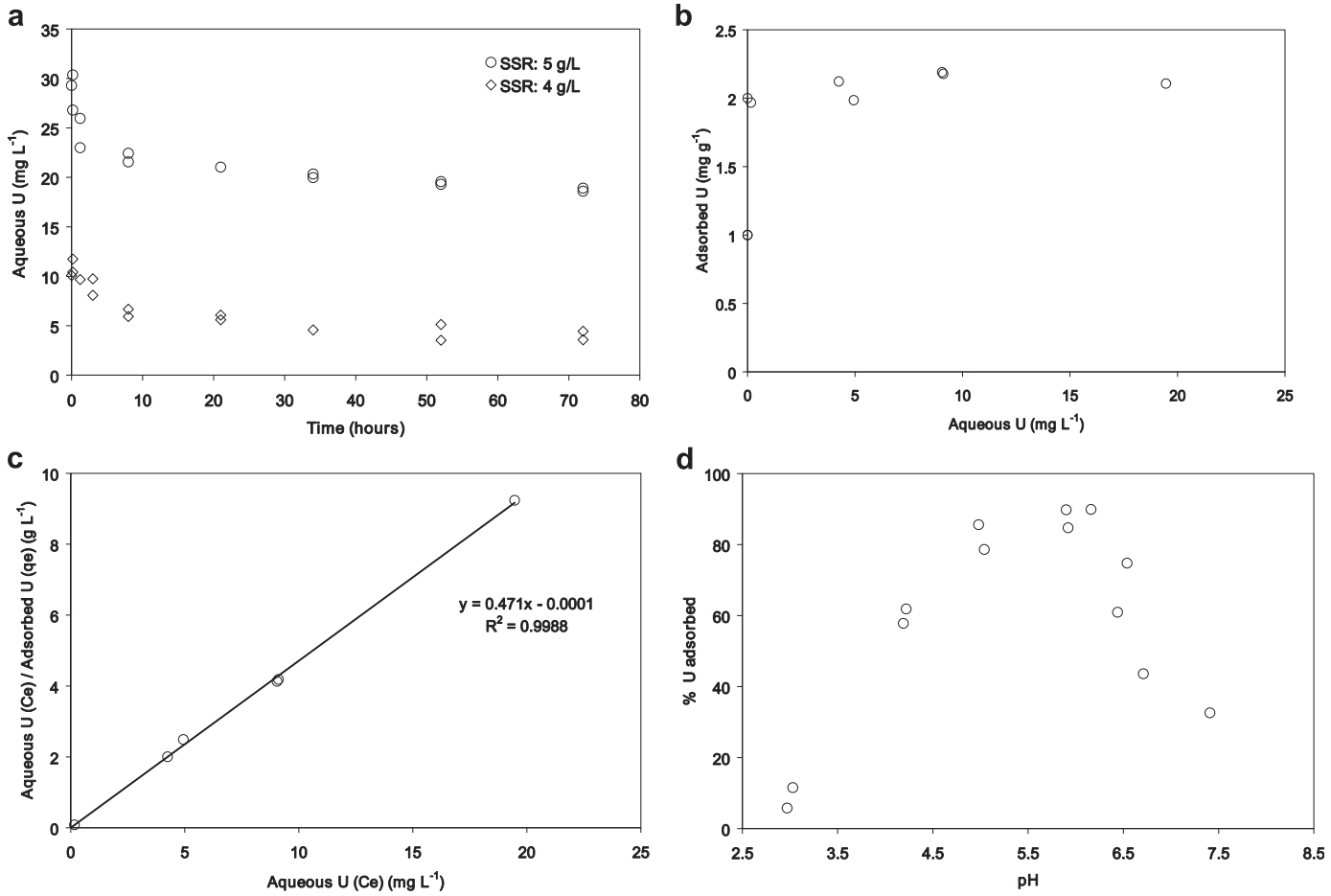

Fig. 3. (a) Kinetics of U(VI) adsorption onto biochar at different solid loadings (SSR: grams of biochar per litre) and initial U(VI) concentrations. pH: 3.9 ± 0.2; ionic strength: 0.1 M $NaNO_3$. (b). Adsorption isotherm of U(VI) onto biochar. SSR: 5 g L^{-1} pH: 3.9 ± 0.2; ionic strength: 0.1 M $NaNO_3$. (c). Adsorption isotherm of U(VI) onto biochar. SSR: 5 g L^{-1} pH: 3.9 ± 0.2; ionic strength: 0.1 M $NaNO_3$. Isotherm data in Fig. 3b fitted using Langmuir model. (d) Adsorption of U(VI) onto biochar with respect to pH. Total U(VI): 30 ppm. Ionic strength: 0.1 M $NaNO_3$.

6.2 resulted in decreasing adsorption. These results indicate that adsorption of U(VI) on to biochar was highly dependent on U(VI) speciation.

The speciation of uranium with respect to pH at 20 mg L^{-1} in 0.1 M $NaNO_3$ system was calculated using Visual MINTEQ 3.0 (Fig. S4, supporting information). At low pH, the biochar surface was expected to be protonated and hence positively charged (<pH 3.5). Hence, adsorption of UO_2^{+2} ions was less preferred at low pH. An increase in pH resulted in a less positive biochar surface that adsorbed the cationic uranium species [$(UO_2)_2(OH)_2^{+2}$, UO_2OH^+, $(UO_2)_3(OH)_5^+$]. Around the circumneutral pH, U(VI) speciation was dominated by anionic uranyl carbonate [$(UO_2)_2CO_3(OH)^{3-}$, $UO_2(CO_3)_3^{4-}$, $UO_2(CO_3)_2^{2-}$] and hence adsorption onto biochar decreased beyond pH 6.2. These results indicate that by adjusting the solution pH, the adsorption efficiency of biochar could be optimized.

5.3. Column adsorption results

The permeable reactive barrier setup is shown in Fig. S5 (supporting information). The U(VI) breakthrough from the PRB column indicated a biochar adsorption capacity of 0.52 mg U g^{-1} of biochar (Fig. 4a). When compared to the adsorption of U(VI) onto quartz at similar conditions (Fig. 4b), U(VI) adsorbed to biochar was 473 times more, on unit mass basis. Though the U(VI) adsorption capacity for biochar observed in the PRB column was about four times less than what was observed in the batch adsorption experiment, it was still significantly higher than pure quartz. Moreover, the low U(VI) adsorption onto biochar in the column setting (relative to the results expected from the batch experiments) could be due to preferential flow scenarios in the column resulting in lesser reactive surface when compared to batch conditions. Furthermore, in the PRB column, the adsorbent material, biochar,

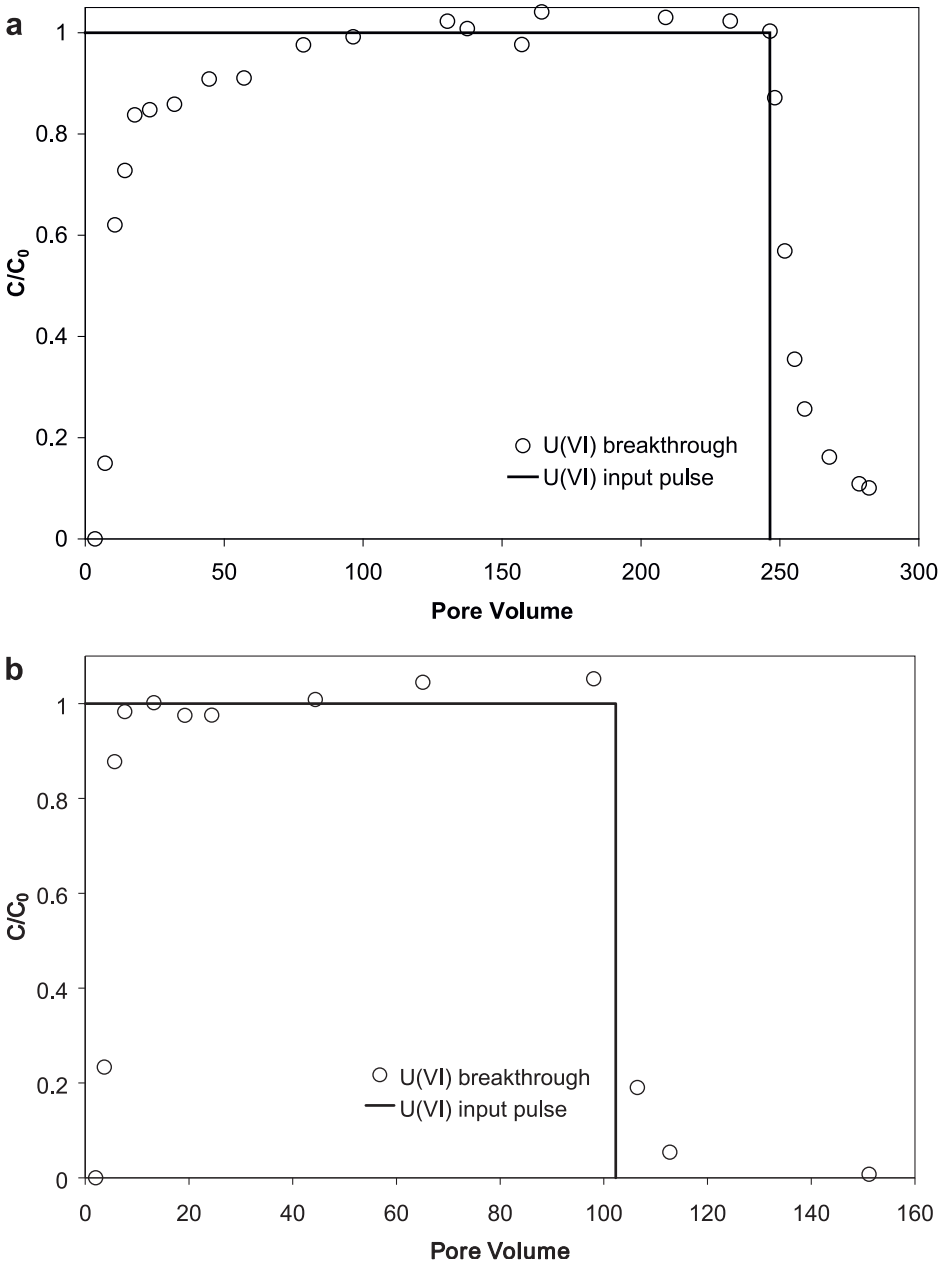

Fig. 4. (a) U(VI) breakthrough profile in a column wherein biochar was used as a PRB medium. C_0: 3 mg L^{-1}; pH: 3.9 ± 0.2; I: 0.1 M $NaNO_3$. (b) U(VI) breakthrough profile in a column filled with pure quartz, serves as a control for PRB column. C_0: 3 mg L^{-1}; pH: 3.9 ± 0.2; I: 0.1 M $NaNO_3$.

was packed to a depth of about 0.80 cm which is similar to the thickness of the column itself 1.0 cm. Hence, a relatively lesser U(VI) adsorption to biochar was expected in the column setting when compared to the batch setting due to considerable loss of reactive surface to the glass column surface. However, the experimental conditions for U(VI) adsorption can be optimized for maximum U(VI) removal, by increasing the pH (Fig. 3d).

Liu and Zhang (2009) reported a similar trend in adsorption for Pb(II) and Cu(II) binding onto the biochar produced via hydrothermal treatment. They showed that the adsorption was a physical endothermic process where irregular oxygen-containing surfaces proved to be beneficial. They further compared the adsorption properties of biochar produced via the hydrothermal carbonization and pyrolysis process. For the case of copper removal from wastewater, it was concluded that the biochar produced from HTC showed better adsorption properties (4.46 mg g^{-1}) than that from pyrolysis (2.75 mg g^{-1}) (Liu et al., 2010). Contrary to the hydrothermal process, pyrolysis resulted in much less oxygen-containing groups on the biochar surface due to deeper carbonization of biomass. The sorption properties of these materials are due to the presence of functional groups such as carboxyl, carbonyl, and hydroxyl, which have a high affinity for metal ions.

A recent review shows the importance of adsorbent materials (activated carbon, ionic exchange resins, zero-valent iron, etc.) as a permeable reactive barrier (PRB) to treat U(VI)-contaminated groundwater (Maria et al., 2009). The results of this study show that biochar could be considered as a potentially competitive low cost and efficient PRB medium for U(VI). Moreover, it would also provide the opportunity for long-term storage of carbon in soil (Shrestha et al., 2010). Besides being free of toxic or carcinogenic compounds, the carbonaceous material is also water-wettable. In view of the growing biofuels industry, it is important to add value to the byproduct, biochar, collected at the end of bioenergy cycle. If not utilized properly, biochar can be an atmospheric pollutant (Shrestha et al., 2010). The effective use of biochar for contaminant remediation would also enhance the goal of the green processes. Considering the cost factor, biochar produced via the HTC process is relatively less energy intensive and can be viewed as a potential low cost process for obtaining efficient adsorbents. Moreover, when compared to other PRB medium, for example zero-valent iron, biochar is expected to be more stable under changing redox conditions. When compared to bone char or apatite which sequesters U(VI) by forming stable uranyl precipitates, biochar entraps U(VI) by sorption mechanism even at low pH as encountered in many U(VI) contaminated sites (Bostick et al., 2002). These properties of biochar support its utility as a highly beneficial contaminant remediation strategy.

6. Conclusions

This study indicates that hydrothermally produced biochar is a porous and amorphous solid rich in active functional groups (hydroxyl/phenolic, carboxylic, and carbonyl groups). The adsorption of uranium onto biochar is an attractive alternative to treat U(VI)-contaminated groundwater. The kinetics of the sorption process was fast and the extent of adsorption resembles an H-type isotherm. Moreover, the adsorption capacity is highly dependent on the system pH. A column experiment supported the use of biochar as a permeable reactive barrier medium. Compared to other remediation strategies, the feasibility of biochar as U(VI) adsorbent is supported by its environmentally benign nature. The major advantage of biochar is that it could serve as an effective and green adsorbent for U(VI) without causing environmental damages.

Acknowledgments

The authors would like to thank Mr. Adam Byrd, Department of Chemical Engineering, Auburn University, Auburn, AL, for the help with the BET analysis. The authors also appreciate the assistance of Mr. William Wills, Soil Testing Laboratory, Auburn, AL, in the elemental analysis work. The authors are thankful for the financial supports from the National Science Foundation (grant NSF-CBET-0828269), the Office of Science, (BER), U.S. Department of Energy, and Alabama Center for Paper and Bioresource Engineering.

Appendix. Supplementary material

Supplementary data associated with this article can be found, in the online version, at doi:10.1016/j.jenvman.2011.05.013.

References

Amuda, O.S., Giwa, A.A., Bello, I.A., 2007. Removal of heavy metal from industrial wastewater using modified activated coconut shell carbon. Biochem. Eng. J. 36, 174–181.
Antal, M.J.Jr., Mochidzuki, K., Paredes, L.S., 2003. Flash carbonization of biomass. Ind. Eng. Chem. Res. 42, 3690–3699.
Aytas, S., Akyil, S., Aslani, M.A.A., Aytekin, U., 1999. Removal of uranium from aqueous solutions by diatomite. J. Radioanal. Nucl. Ch 240, 973–976.
Baeza, J., Freer, J., 2001. Chemical Characterization of Wood and Its Components, P. 275–384. In: Hon, DN.-S., Shiraishi, N. (Eds.), Wood and Cellulosic Chemistry, second ed. Marcel Dekker, Inc., New York. Basel.
Berg, D.V.D., Visser, P.D., 2001. "Switchgrass". BTG (Biomass Technology Group). Final Report FAIR 5-CT97-3701. Enschede, The Netherlands (Chapter 7), pp. 48–50.
Brown, R.C., 2008. Biochar Production Technology, Center for Sustainable Environmental Technologies. Department of Mechanical Engineering, Iowa State University. www.bioeconomyconference.org/.../Brown,%20Richard.pdf – http://www.bioeconomyconference.org/08%20Presentations%20approved/Breakouts/Biomass%20Processing/Brown,%20Richard.pdf.
Bostick, B.C., Fendorf, S., Barnett, M.O., Jardine, P.M., Brooks, S.C., 2002. Uranyl surface complexes formed on subsurface media from DOE facilities. Soil Sci Soc Am J 66, 99–108.
Budinova, T., Ekinci, E., Yardim, F., Grimm, A., Bjornbom, E., Minkova, V., Goranova, M., 2006. Characterization and application of activated carbon produced by H3PO4 and water vapor activation. Fuel Process. Technol. 87, 899–905.
Camacho, L.M., Deng, S., Parra, R.R., 2010. Uranium removal from groundwater by natural clinoptilolite zeolite: Effects of pH and initial feed concentration. J. Hazard. Mater. 175, 393–398.
Cao, X., Ma, L., Gao, B., Harri, W., 2009. Dairy-Manure derived biochar Effectively sorbs lead and Atrazine. Environ. Sci. Technol. 43, 3285–3291.
Chen, B., Chen, Z., 2009. Sorption of naphthalene and 1-naphthol by biochars of orange peels with different pyrolytic temperatures. Chemosphere 76, 127–133.
Chen, B., Zhou, D., Zhu, L., 2008. Transitional adsorption and partition of nonpolar and polar aromatic contaminants by biochars of pine needles with different pyrolytic temperatures. Environ. Sci. Technol. 42, 5137–5143.
Cheng, L., Ye, X.P., He, R., Liu, S., 2009. Investigation of rapid conversion of switchgrass in subcritical water. Fuel Process. Technol. 90, 301–311.
Dachs, J., 2000. Adsorption onto aerosol soot carbon dominates gas-particle partitioning of polycyclic aromatic hydrocarbons. Environ. Sci. Technol. 34, 3690.
Davis, J.A., Meece, D.E., Kohler, M., Curtis, G.P., 2004. Approaches to surface complexation modeling of Uranium(VI) adsorption on aquifer sediments. Geochim. Cosmochim. Ac 68, 3621–3641.
Ervanne, H., 2003. Interferences in uranium oxidation states during dissolution of solid phases. J. Radioanal. Nucl. Ch 256, 497–500.
Funke, A., Ziegler, F., 2010. Hydrothermal carbonization of biomass: a summary and discussion of chemical mechanisms for process engineering. Biofuel. Bioprod. Bior. 4, 160–177.
Gaunt, J.L., Lehmann, J., 2008. Energy balance and emissions associated with biochar sequestration and pyrolysis bioenergy production. Environ. Sci. Technol. 42, 4152–4158. http://www.biochar-international.org/biochar [Online] (verified February, 2010).
Hu, B., Yu, S.-H., Wang, K., Liu, L., Xu, X.-W., 2008. Functional carbonaceous materials from hydrothermal carbonization of biomass: an effective chemical process. Dalton T. 40, 5414–5423.
Isaac, R.A., Johnson, W.C., 1985. Elemental analysis of plant Tissue by Plasma Emission spectroscopy: Collaborative study. J. Assoc. Off. Anal. Chem. 68 (3), 499–505.
Kalderis, D., Koutoulakis, D., Paraskeva, P., Diamadopoulos, E., Otal, E., Valled, J.O., Fernandez-Pereira, C., 2008. Adsorption of polluting substances on activated carbons prepared from rice husk and sugarcane bagasse. Chem. Eng. J., 144.
Karaosmanoglu, F., Isıgjıgur-Ergudenler, A., Sever, A., 2000. Biochar from the straw-stalk of rapeseed plant. Energ. Fuels 14, 336–339.

Kirsten, W.J., 1979. Automated Methods for the determination of carbon, hydrogen, nitrogen, and sulfur, and sulfur alone in organic and inorganic materials. Anal.Chem 51, 1173–1179.
Kobayashi, N., Okada, N., Hirakawa, A., Sato, T., J.KobayashiHatano, S., Itaya, Y., Mori, S., 2009. Characteristics of solid residues obtained from hot-compressed-water treatment of woody biomass. Ind. Eng. Chem. Res. 48, 373–379.
Kumar, S., 2010. Dissertation on "Hydrothermal Treatment for Biofuels: Lignocellulosic Biomass to Bioethanol, Biocrude, and Biochar". Department of Chemical Engineering, Auburn University, Auburn, AL, USA.
Kumar, S., Gupta, R.B., 2009. Biocrude production from switchgrass using subcritical water. Energ. Fuels 23, 5151–5159.
Laird, D.A., Brown, R.C., Amonette, J.E., Lehmann, J., 2009. Review of the pyrolysis platform for coproducing bio-oil and biochar. Biofuel. Bioprod. Bior 3, 547–562.
Lehmann, J., 2007. Bio-energy in the black. Front. Ecol. Environ. 5, 381–387.
Limousin, G., Gaudet, J.P., Charlet, L., Szenknect, S., Barthes, V., Krimissa, M., 2007. Sorption isotherms: a review on physical bases, modeling and measurement. Appl. Geochem. 22, 249–275.
Liu, Z., . Zhang, F.-S., 2009. Removal of lead from water using biochars prepared from hydrothermal liquefaction of biomass. J. Hazard. Mater. 167, 933–939.
Liu, Z., Zhang, F.-S., Wu, J., 2010. Characterization and application of chars produced from pinewood pyrolysis and hydrothermal treatment. Fuel 89, 510–514.
Loganathan, V.A., Feng, Y.C., Sheng, G.D., Clement, T.P., 2009. Crop-Residue-Derived char influences sorption, Desorption and Bioavailability of Atrazine in soils. Soil Soc. Am. J. 73, 967–974.
Maria, G., Vasile, P.L., Igor, C., 2009. Characterization and remediation of soils contaminated with uranium. J. Hazard. Mater. 163, 475–510.
McKay, J.F.P.G., 1997. Equilibrium parameters for the sorption of copper, cadmium and zinc ions onto peat. J. Chem. Technol. Biotechnol. 69, 309–320.
Mellah, A., Chegrouche, S., Barkat, M., 2006. The removal of uranium(VI) from aqueous solutions onto activated carbon: kinetic and thermodynamic investigations. J. Colloid Interf. Sci. 296, 434–441.
National Biofuels Action Plan. October, 2008. http://www1.eere.energy.gov/biomass/pdfs/nbap.pdf.
Parab, H., Joshi, S., Shenoy, N., Verma, R., Lali, A., Sudersanan, M., 2005. Uranium removal from aqueous solution by coir pith: equilibrium and kinetic studies. Bioresour. Technol. 96, 1241–1248.
Patrick, H.R., Griffith, K., Liotta, C.L., Eckert, C.A., 2001. Near critical water: a benign medium for catalytic reactions. Ind. Eng. Chem. Res. 40, 6063–6067.
Perlack, R.D., Wright, L.L., Turhollow, A.F., Graham, R.L., Strokes, B.J., Erbach, D.C., 2005. Biomass as a feedstock for a bioenergy and bioproducts industry: the technical feasibility of a billion-ton annual supply. A Joint report sponsored by U.S. Department of Energy and U.S. Department of Agriculture. 78.
Psarevaa, T.S., Zakutevskyya, O.I., Chubara, N.I., Strelkoa, V.V., Shaposhnikovaa, T.O., Carvalhob, J.R., Correia, M.J.N., 2005. Uranium sorption on cork biomass. Colloid Surf. A 252, 231–236.
Savovaa, D., Apakb, E., Ekincib, E., Yardimb, F., Petrova, N., Budinovaa, T., 2001. Biomass conversion to carbon adsorbents and gas. Biomass Bioenerg. 21, 133–142.
Sciban, M., Radetic, B., Kevresan, Z., Klasnja, M., 2007. Adsorption of heavy metals from electroplating wastewater by wood sawdust. Bioresour. Technol. 98, 402–409.
Segal, L., Creely, J.J., Martin, A.E., Conrad, C.M., 1959. An empirical method for estimating the degree of crystallinity of native cellulose using the X-ray diffractometer. Textile Res. J. 29, 786–794.
Sevilla, M., Fuertes, A.B., 2009. The production of carbon materials by hydrothermal carbonization of cellulose. Carbon 47, 2281–2289.
Shrestha, G., Traina, S.J., Swanston, C.W., 2010. Black carbon's properties and role in the environment: a comprehensive review. Sustainability 2, 294–320.
Smernik, R.J., 2009. Biochar and sorption of organic compounds, p. 289–300. In: Lehmann, J., Joseph, A. (Eds.), Biochar for Environmental Management: Science and Technology. Earthscan, London.
Srivastava, S., Bhainsa, K.C., D'Souza, S.F., 2010. Investigation of uranium accumulation potential and biochemical responses of an aquatic weed Hydrilla verticillata (L.f. Royle. Bioresour. Technol. 101, 2573–2579.
Suhas, P.J.M.C., Carrott, M.M.L.R., 2007. Lignin-from natural adsorbent to activated carbon: a review. Bioresour. Technol 98, 2301–2312.
Tan, W.T., Ooi, S.T., Lee, C.K., 1993. Removal of Cr(VI) from solution by coconut husk, palm pressed fibers. Environ. Technol. 14, 277–282.
Titirici, M.M., Thomas, A., Antonietti, M., 2007. Back in the black: hydrothermal carbonization of plant material as an efficient chemical process to treat the CO_2 problem. New J. Chem. 31, 787–789.
Vandenhovea, H., Cuypersb, A., Heesa, M.V., Koppenc, G., Wannijna, J., 2006. Oxidative stress reactions induced in beans (Phaseolus vulgaris) following exposure to uranium. Plant Physiol. Bioch 44, 795–805.
Winsley, P., 2007. Biochar and bioenergy production for climate change. Mitigation. NZ Sci. Rev. 64, 5–10.
Yu, X.Y., Ying, G.G., Kookana, R.S., 2009. Reduced plant uptake of pesticides with biochar additions to soil. Chemospere 76, 665–671.
Zeng, H., Singh, A., Basak, S., Ulrich, K.-U., Sahu, M., Biswas, P., Catalano, J.G., Giammar, D.E., 2009. Nanoscale size effects on uranium (VI) adsorption to hematite. Environ Sci Technol. 43, 1373–1378.